Cerebral Cortex October 2007;17:2433-2442
doi:10.1093/cercor/bhl151
Advance Access publication January 4, 2007

# Computational Models of Neocortical Neuronogenesis and Programmed Cell Death in the Developing Mouse, Monkey, and Human

Julia M. Gohlke[1], William C. Griffith and Elaine M. Faustman

Department of Environmental and Occupational Health Sciences, University of Washington, Seattle, WA 98105, USA
[1]Current address: Environmental Systems Biology Group, Laboratory of Molecular Toxicology, National Institute of Environmental Health Sciences, RTP, NC 27709, USA

**This paper presents a computational model allowing quantitative simulations of acquisition of neocortical neuronal number across mammalian species. When extrapolating scientific findings from rodents to humans, it is particularly pertinent to acknowledge the importance of the accelerated enlargement of the neocortex during human evolution. Neocortex development is marked by discrete stages of neural progenitor cell proliferation and death, neuronal differentiation, and neuronal programmed cell death. We have developed computational models of human and rhesus monkey neocortical neuronal cell acquisition based on experimentally derived parameters of cell cycle length, commitment to cell cycle exit, and cell death. Our model results agree with independent stereological studies estimating neocortical neuron number in adult and developing rhesus monkey and human. Comparisons of our primate models with previously developed rodent models suggest correlations between the lengthening of the duration of the neuronogenesis period and a lengthening of the cellular processes of cell cycle progression and death can account for the vast increase in size of the primate neocortex. Furthermore, when compared with rodents, we predict that cell death may play a larger role in shaping the primate neocortex. Our mathematical models of the development and evolution of the neocortex provide a quantitative, biologically based construct for extrapolation between rodent and humans. These models can assist in focusing future experimental research on the differing mechanisms of rodent versus human neocortical development.**

**Keywords:** apoptosis, cell cycle, evolution, mathematical model, neuron number, rhesus

## Introduction

A defining feature in the evolution of primates is the remarkable increase in the size of the neocortex, the thin, layered sheet of neurons on the dorsal surface of the brain (Northcutt and Kaas 1995). Across mammalian species, there is a massive amount of variation in the absolute and relative size of the neocortex. The neocortex can occupy anywhere from 25% to 80% of the brain, even though the overall cellular architecture is conserved in all mammals (Clark et al. 2001). Although a large increase in the relative size of the neocortex is evident in the evolution of primates and some other mammals such as cetaceans, the relative size of other brain regions, such as the cerebellum and hippocampus, stays constant or becomes smaller in proportion to total brain size (Hofman 1982; Clark et al. 2001). In fact, neocortical surface area increases 100 times from mouse to monkey, and 1000 times from mouse to human, however, the thickness of the neocortex stays constant or increases only slightly (approx. 2 times) (Rockel et al. 1980; Rakic 1995).

The overall progression of neocortical development is amazingly well conserved across species, despite the large variations in size and specializations that occur in adults (Hendry et al. 1984; Smart 1991; Bayer et al. 1993; Kornack 2000; Clancy et al. 2001). The beginning of neurogenesis is marked by the first asymmetric division of progenitor cells, forming one young postmitotic neuron and one progenitor cell that continues proliferating. As neurogenesis proceeds, a higher percentage of cells exit the cell cycle and become young postmitotic neurons that begin migration out of the ventricular zone (VZ), through the intermediate zone to the cortical plate (CP). The first neurons are generated form the inner layers of the neocortex, whereas additional layers are formed by young neurons migrating past the previous layers, referred to as an inside-out pattern of layer formation. Autoradiographic and retroviral lineage analyses in mouse and monkey and histological studies in humans suggest that this process of neurogenesis begins at E11 in the mouse, E40 in the rhesus monkey, and about E42 in humans (Rakic 1974; Rakic and Kornack 2001; Caviness et al. 2003). The duration of neurogenesis is greatly extended in both humans (approximately 84 days) and monkeys (approx. 60 days) (Rakic 1988) compared with the mouse (approx. 6 days) (Smart and Smart 1977; Takahashi et al. 1997) and rat (7 days) (Bruckner et al. 1976; Lund and Mustari 1977; Nowakowski et al. 1989; Bayer et al. 1993). These data suggest that a stable progression of neuronogenesis is tied to a variable length of neuronogenesis across species. This relationship has been used to explain the observation that late-generated structures with an inside-out pattern of layer formation, such as the neocortex, can evolve to become disproportionately large (Finlay and Darlington 1995; Finlay et al. 1998, 2001; Marin-Padilla 1998).

Programmed cell death also plays a major role in shaping the mammalian neocortex. A well-supported hypothesis suggests that in postmitotic neurons, concurrent with synaptogenesis, an elimination process occurs in neurons not making correct connections. These neurons are not reinforced with trophic support and are deleted via apoptosis (Cowan et al. 1984; Raff et al. 1993). Cell death also plays a role in the proliferative zones of the developing cortex (Chun 2000). In humans and rodents, apoptotic nuclei are very rare during neocortical development (Simonati et al. 1997). However, it is not known whether similar percentages of death labeled cells at any one time correlate to a similar relative reduction in the number of cells in the final structure. Indeed, determination of the total number of cells that die based on histological counts of dying cells is a particularly difficult task because the length of time between label acquisition and complete clearance of death labeled cells is hard to ascertain and is dependent on whether the detection method is an early or late marker of cell death (Voyvodic 1996).

© The Author 2007. Published by Oxford University Press. All rights reserved.
For permissions, please e-mail: journals.permissions@oxfordjournals.org

Downloaded from http://cercor.oxfordjournals.org/ at University of North Texas on January 5, 2017

As biomedical research routinely relies on the rodent model, an appreciation of the evolutionary changes in the cellular mechanisms of neocortical development is necessary in order for us to delineate how specific perturbations during development may cause long-term neocortical-related deficits in humans. We have previously built computational models for rat and mouse neocortical development from the production of neurons during neuronogenesis through the normal loss of young neurons during synaptogenesis to form the final population of neurons in the adult neocortex (Gohlke et al. 2002, 2004). In addition, we have applied these models to quantitatively described the impact of ethanol-induced inhibition of the cell cycle and induction of cell death on neocortical neuronal number (Gohlke et al. 2002, 2005). Using the same underlying mathematical construct, here we develop models of rhesus monkey and human neocortical development. We base our models on specific experimental studies in monkeys and humans, which measure the length of neuronogenesis, the cell cycle length, and the amount of cells labeled for death during neocortical development.

The theory of heterochrony, or changes in the rate or sequence of developmental events, offers an evolutionary context in which to explain diversity in size and shape based on the lengthening or shortening of developmental processes, such as is evident with the evolution of the neocortex. The overall lengthening of the duration of the neuronogenesis period in primate species compared with rodent species may be dependent on lengthening of cellular processes, such as the rate of cell cycle progression and rate of programmed cell death. For example, sequential S phase labeling during neocortical neuronogenesis in the rhesus monkey and rodent species suggesting that the cell cycle length is much longer in primates supports this hypothesis (Miller and Kuhn 1995; Takahashi et al. 1995; Kornack and Rakic 1998). However, it is unknown whether lengthening of the process of cell death also occurs in primate species. We explore the theory of heterochrony among species as it relates to the evolution of the neocortex by building rate-adjusted models based on the assumption that both the cell cycle progression and death rates are proportional to the duration of neuronogenesis across species. We compare numbers generated from our models with data generated from independent stereological studies of adult neocortical neuron numbers in the rhesus monkey and human.

## Methods

Using the general model framework of Leroux et al. (1996), we have developed time-extrapolated models of monkey and human neocortical development based, in part, on our previous model for mouse neocortical development (Gohlke et al. 2002, 2004), and key evolutionary parameters such as the increased length of the neuronogenesis period and cell cycle length in the primate (Fig. 1; Table 1). We established rates of cell cycle progression and death for the human and monkey based on the experimentally determined cell cycle lengths in the rhesus monkey (Kornack and Rakic 1998) and experimentally determined % of TUNEL(+) (terminal deoxynucleotidyl transferase biotin–deoxy uridine triphosphate [dUTP] nick end labeling) cells over time in the human fetus (Chan and Yew 1998; Rakic and Zecevic 2000). We compared these with our previously developed mouse model rates (Fig. 2*A* and *C*). Neuronal differentiation can be quantitatively estimated based on experiments determining the percent of cells becoming postmitotic, or the *Q* (quiescent) fraction, on each day of neuronogenesis in the psuedostratified ventricular epithelium (PVE) mouse (Takahashi et al. 1996), as these postmitotic cells leaving the PVE subsequently migrate to the CP, where they differentiate into neurons. Therefore, the

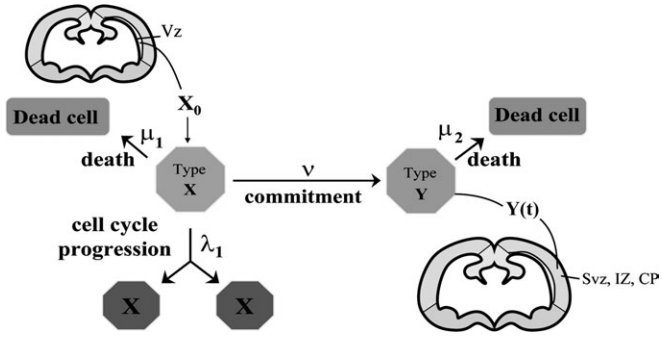


**Figure 1.** Critical parameters for primate neocortical neuronogenesis models. This diagram shows key parameters for mouse, monkey, and human neocortical neuronogenesis models as they relate to the original framework for a computational model for developmental processes proposed by Leroux et al. (1996). Mouse neocortical neuronogenesis lasts approx. 6 days (Takahashi et al. 1995), whereas monkey lasts approx. 60 and human lasts approx. 84 days (Rakic 1988; Kornack and Rakic 1998). The starting cell number ($X_0$) in the primate models is approx. 4 times that of the mouse (Caviness et al. 1995), the cell cycle progression rate ($\lambda_1$) of precursor (*X*) cells is approx. 2–4 times slower in primate models (Kornack and Rakic 1998), and the cell death rates ($\mu_1$ and $\mu_2$)and commitment rate (ν) from *X* cells to committed neuronal (*Y*) cells are comparable across species (Caviness et al. 1995; Rakic and Zecevic 2000). IZ, intermediate zone.

commitment to exit the cell cycle is a parameter in our model estimating subsequent differentiation into a neuronal lineage. The cell cycle exit commitment rate is also dependent on the cell cycle length, which does vary between species and therefore varies the cell cycle exit commitment rate slightly across species (Fig. 2*B*). Numerous reports suggest a similar progression of the *Q* fraction over the neuronogenesis period in various species (Caviness et al. 1995; Kornack 2000).

### *Generalized Model Construct*

The general model construct has been described previously (Leroux et al. 1996; Faustman et al. 1999; Gohlke et al. 2002, 2004). In our model of neocortical development (Gohlke et al. 2002, 2004), the X cell represents progenitor cells in the ventricular epithelium that have the potential to divide, differentiate into a Y cell, or die. The Y cell represents a postmitotic, young neuron, therefore, the Y cell cycle progression rate is set to zero. Two assumptions of the underlying mathematical construct are 1) commitment to differentiate from an X cell to a Y cell is irreversible in that a committed postmitotic neuron leaving the ventricular region does not have the potential to revert back to a proliferating progenitor cell and 2) all cells are assumed to act independently of each other.

To derive the mathematical properties of the model, let $X(t)$ and $Y(t)$ denote the numbers of X and Y cells at time $t$, respectively. Then a transition probability can be defined as

$$P(x, y, t; x_o, y_o, t_o) = P(X(t) = x, Y(t) = y | X(t_o) = x_o, Y(t_o) = y_o). \quad (1)$$

The initial time $t_o$ represents the beginning of neuronogenesis, so that the number of type Y cells initially present will be $y_o = 0$. We use a Kolmogorov forward equation to describe the transition probabilities:

$$\begin{aligned} dP(x, y, t)/dt = {} & (x-1)\lambda_1(t)P(x-1, y, t) + (x+1)\mu_1(t)P(x+1, y, t) \\ & + (y-1)\lambda_2(t)P(x, y-1, t) + (y+1)\mu_2(t)P(x, y+1, t) \\ & + (x+1)\nu(t)P(x+1, y-1, t) - [x\lambda_1(t) + x\mu_1(t) + y\lambda_2(t) \\ & + y\mu_2(t) + x\nu(t)]P(x, y, t). \end{aligned} \quad (2)$$

When the number of X cells initially present is large, the distribution of ($X(t)$, $Y(t)$) is approximately bivariate normal by the central limit theorem. Therefore, the moments, or the numbers of X and Y cells at time ($t$) can be derived through the first-order differential equation and



Downloaded from http://cercor.oxfordjournals.org/ at University of North Texas on January 5, 2017

**Table 1**
Experimental data for parameterization of neocortical development models

| | Reference | Model parameter | Description | Phase 1 model | Phase 2 model |
|---|---|---|---|---|---|
| Mouse experimental data | | | | | |
| Cell cycle length ($T_c$) on E11–E16 | (Takahashi et al. 1995) | $\lambda_1$ | X-cell cell cycle progression rate | Figure 2(*A*) (mouse only) | Figure 3(*C*) (Eqs. 9, 10) (monkey and human) |
| Quiescent fraction (*Q*) on E11–E16 | (Takahashi et al. 1996) | $\nu_0$ | X–Y commitment rate | Figure 2(*B*) (Eqs. 5, 6) (mouse, monkey, and human) | Figure 3(*B*) (Eqs. 5, 6) |
| % TUNEL(+) on E15–18 | (Hoshino and Kameyama 1988; Verney et al. 2000) | $\mu_1$ | X cell death rate | Figure 2(*C*) (mouse only) | — |
| % TUNEL(+) on P1–P14 | (Hoshino and Kameyama 1988; Verney et al. 2000) | $\mu_2$ | Y cell death rate | Figure 2(*C*) (mouse only) | — |
| Clearance time of apoptotic cells in developing forebrain on E19 | (Thomaidou et al. 1997) | $\mu_1$ and $\mu_2$ | X and Y cell death rate | Figure 2(*C*) (Eq. 7) (mouse, monkey and human) | Figure 3(*B*) (Eqs. 9, 10) (monkey and human) |
| # of neurons in PVE on E11 | (Caviness et al. 1995; Haydar et al. 2000) | $X_0$ | Initial # of X cells | Equation (1) (mouse, monkey and human) | Equation (11) (human) |
| Monkey experimental data | | | | | |
| Cell cycle length ($T_c$) on E40, E60, and E80 | (Kornack and Rakic 1998) | $\lambda_1$ | X-cell cell cycle progression rate | Figure 2(*A*) (Eq. 3) (monkey and human) | Figure 3(*A*) (Eq. 8) (human) |
| Human experimental data | | | | | |
| % TUNEL(+) for weeks 6–32 | (Rakic and Zecevic 2000) | $\mu_1$ and $\mu_2$ | X and Y cell death rate | Figure 2(*C*) (Eq. 7) (monkey and human) | Figure 3(*C*) (Eqs. 7, 9, 10) (monkey and human) |

can be approximated through a solution matrix described previously (Leroux et al. 1996; Gohlke et al. 2002).

### *Primate Models of Neocortical Neuronal Acquisition (Phase 1)*

The founder X cell population ($X_0$), or the number of cells present at the beginning of neuronogenesis, has been estimated experimentally in the mouse using stereological techniques (Haydar et al. 2000). Based on the larger monkey fetal brain size, Caviness et al. (1995) estimated the monkey founder cell population is from 4 to 5 times larger than the mouse. Here we have increased the mouse cell founder population (estimated at 500 000 cells) 5-fold to estimate both monkey and human founder cell populations, to give an estimated founder population of 2 500 000 cells. Sensitivity analysis of this parameter has been performed previously in rodent models (Gohlke et al. 2004).

A piecewise constant approach is used in which time steps are employed to accommodate the time varying parameters of neocortical neuronogenesis. Each model has 11 time steps spanning the length of neuronogenesis which has been experimentally determined as spanning approximately 6 days for the mouse (Takahashi et al. 1997), 60 days for the rhesus monkey (Rakic 1974; Kornack and Rakic 1998), and approximately 84 days in the human (Rakic 1978, 1988; Simonati et al. 1999; Chan et al. 2002). The time steps for our mouse model are calculated as the length of each experimentally determined cell cycle (Takahashi et al. 1997), whereas in our primate models, time steps span several days as the length of the neuronogenesis period is considerably longer. No difference in output was seen when we increased the number of time steps (up to 100) in our primate models.

Our primate models have an X cell cycling rate ($\lambda_1$) based on the cell cycle length data at E40, E60, and E80 in the rhesus monkey (Kornack and Rakic 1998). Although this is the only study determining actual cell cycle lengths, other studies using proliferation cell nuclear antigen (an auxillary protein of DNA polymerase $\delta$ which is expressed during the G1 to S transition) in human fetal tissue or single injections of [$^3$H] thymidine done in the rhesus monkey offer semiquantitative support of these results (Dehay et al. 1993; Mollgard and Schumacher 1993; Simonati et al. 1999). A linear extrapolation was used to determine cell cycle lengths between E40 and E60 and E60 and E80. Between E80 and E100 a constant cell cycle length was used based on the E80 experimental datum. We are using an exponential function to describe a cell cycle progression rate based on the amount of time it takes for a cell population to double. Cell cycle length ($T_c$) was then used to calculate a monkey specific cell cycle progression rate ($\lambda_{mon}$) by the following equation:

$$\lambda_{mon}(t) = \ln 2/T_c. \tag{3}$$

The meaning of the rate $\lambda_1(t)$ is that in a small time interval $(t + \Delta t)$ the probability that a type X cell divides is approximately $\lambda_1(t)\Delta t$.

For the human model, the Kornack and Rakic (1998) data were utilized by stretching it over the 84-day neuronogenesis period using the following equation:

$$\lambda_{hum}(t_{hum}) = \lambda_{mon}(t_{hum} - 46) \times (60/84) + 40), \tag{4}$$

where $t_{hum} = (t_{mon} - 40) \times (84/60) + 46$, as the human neurogenesis period starts on day 46 and is approximately 84 days long, whereas the monkey neuronogenesis period starts on day 40 and is approximately 60 days long. This interspecies difference in the cell cycle progression rate ($\lambda_1$) of X cells is shown in Figure 2(*A*).

The commitment rate ($\nu_0$) describing exit from the cell cycle is based on extrapolations of the experimentally determined quiescent fraction (*Q*) in the mouse model (Takahashi et al. 1996). The Y commitment rate ($\nu_0$) is approximated from *Q*, which can be described by

$$Q = Y(t)/(X(t) + Y(t)), \tag{5}$$

where $X(t)$ and $Y(t)$ denote the numbers of type X and type Y cells at time *t*. We then solve for the commitment rate, $\nu_0$, where

$$Y(t)/(X(t) + Y(t)) - Q = 0. \tag{6}$$

We have extended this progression of the cell cycle exit commitment rate in the mouse over the neuronogenesis period in the monkey and human (Fig. 2*B*). Although there are no direct, quantitative data describing the progression of the *Q* fraction in the monkey or human, studies show an increase and subsequent decrease of the cellular content in the VZ that follows that of the mouse, suggesting a similar progression of proliferative fraction (*P*) and *Q* fractions over the neuronogenesis period (Rakic 1988, 1995; Simonati et al. 1999; Chan et al. 2002; Samuelsen et al. 2003). Furthermore, other researchers suggest the progression of *Q* is similar across species based on comparisons of the timing of production of neurons for each layer of the cortex showing identical scaling of the proportion of neuronogenesis that is given to each layer in mouse, rat, cat, and monkey (Caviness et al. 1995; Kornack 2000).

We calculated all death rates for X and Y (proliferative and non-proliferative) cells using TUNEL experimental results. The TUNEL method identifies apoptotic cells in situ by using terminal deoxynucleotidyl transferase to transfer biotin-dUTP to these strand breaks of cleaved DNA. The death rates for X and Y cells ($\mu_1$ and $\mu_2$) are calculated by the following equation:

$$\mu = [(\ln(1 - (\%\,\mathrm{TUNEL}(+)/100))/-1) \times 24\,\mathrm{h}]/\mathrm{CL}, \tag{7}$$

where CL = 2.5 h and represents the duration of label in dying cells using TUNEL staining in the ventricular region of the rat neocortex during neuronogenesis, referred to as the clearance time (Thomaidou et al.

Downloaded from http://cercor.oxfordjournals.org/ at University of North Texas on January 5, 2017

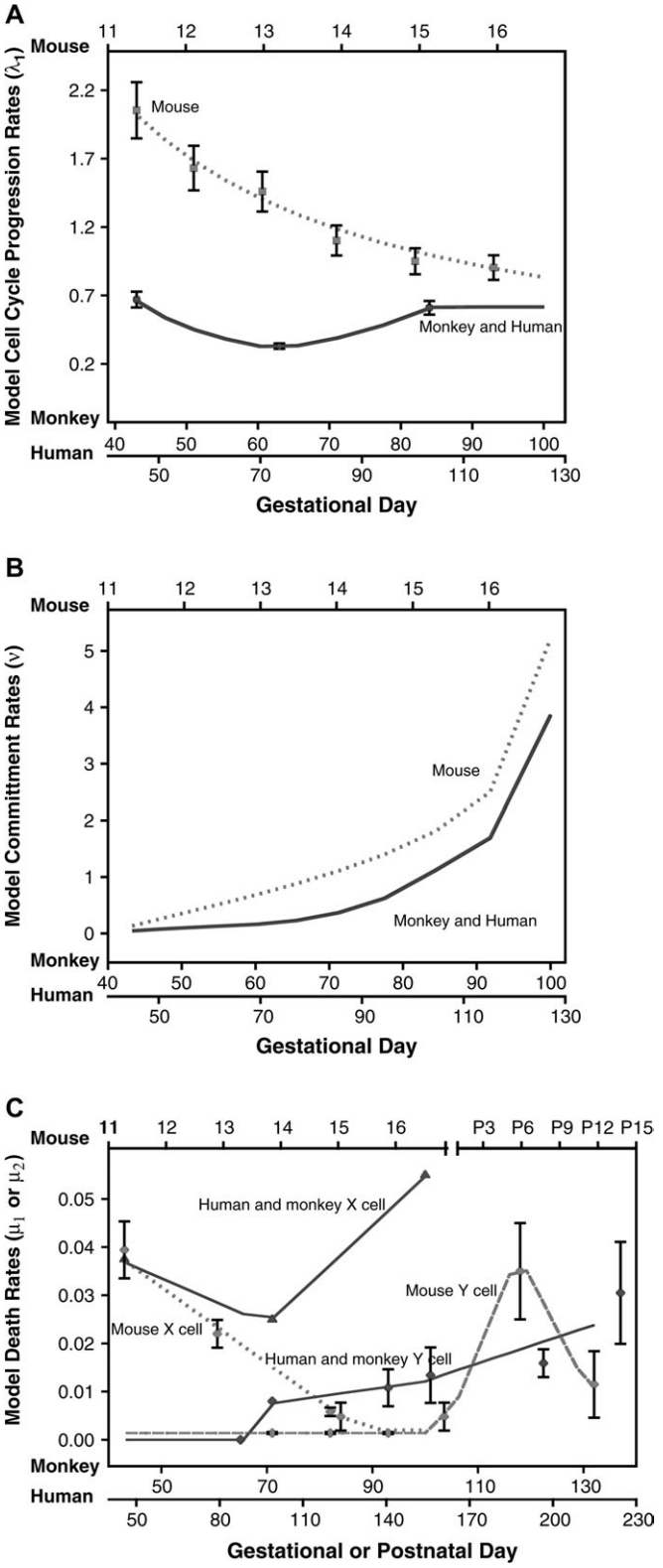


**Figure 2.** Comparison of key time-dependent parameters across mouse, monkey, and human models of neocortical development. (*A*) Cell cycle progression rates in mouse model based on the cell cycle length data of Takahashi et al. (1995) shown as a dotted line. Cell cycle progression rates in monkey and human model based on the cell cycle length data in the monkey (Kornack and Rakic 1998) shown as solid line. (*B*) Commitment rates (ν) based on cell cycle lengths and the fraction of cells becoming postmitotic with each cell cycle (*Q* fraction) determined in the mouse (Takahashi et al. 1997) on E12, E13, E14, and E15 shown as dotted line. Monkey and human predictions shown as dotted line. (*C*) Cell death rates based on percent TUNEL(+) cells in mouse through neuronogenesis (Hoshino and Kameyama 1988) shown as dotted line and synaptogenesis (Verney et al. 2000) shown as dashed line, and human (Chan and Yew 1998; Rakic and Zecevic 2000) from 6 to 32 weeks gestation shown as solid lines. See Methods section for further details and rate equations. Experimental data used to calculate cell cycle progression, commitment, and cell death rates are shown as separate points. Error bars represent standard error of the mean reported in studies.

1997). Although no quantitative analyses of cell death in the monkey developing neocortex are available, we utilized 2 human studies to estimate $\mu_1$ and $\mu_2$ in both the monkey and human models. Chan and Yew (1998) report TUNEL staining at 14, 18, 27, and 32 weeks in the developing human (Chan and Yew 1998). These measurements are supported by Rakic and Zecevic (2000), who report % TUNEL(+) cells in the proliferative VZ and subventricular zone (SVZ) and CP of the developing human at 4.5, 6, 11, 21, and 27 gestational weeks. A linear extrapolation connecting the experimental data points of Rakic and Zecevic (2000) at 6, 11, and 21 gestational weeks in the VZ/SVZ or CP was used to predict % TUNEL(+) cells between experimental time points for cell death determination of X and Y cells, respectively, during the neuronogenesis period in both the monkey and human models. To estimate cell death in Y cells after neuronogenesis during the synaptogenesis period of gestation, a linear extrapolation was performed on the % TUNEL(+) cells in the CP from Chan and Yew (1998) at 18, 27, and 32 weeks and Rakic and Zecevic (2000) at 21 and 27 weeks to predict Y cell death between 18 and 32 weeks in the monkey and human model. Figure 2(*C*) compares our time-dependent death rates from our mouse model (Gohlke et al. 2004) with those used in our primate models.

### *Sensitivity Analyses*

The impact of uncertainty in parameter estimation was explored through several sensitivity analyses. An analysis was performed on the linear extrapolation used for deriving cell cycle lengths based on any 2 points of the monkey cell cycle length ($T_c$) data, as the reduced cell cycle length during the latter portion of neuronogenesis reported in the monkey is inconsistent with rodent data (Fig. 2*A*). This analysis suggests using all 3 data points is the most consistent fit to independent stereological data (Suppl. Fig. S1). A sensitivity analysis of the founder cell population ($X_0$) parameter suggests using a 4-fold rather than a 5-fold increase over the experimentally derived mouse founder population would decrease our projected total output by 23%. However, it is important to note that changing the founder cell population alone does not change estimates of proportional increase or decrease in the cell population over time, as these proportional increases and decreases through time are solely dependent on cell cycle progression, commitment, and death rates. For example, changes in the founder cell population would change the predicted absolute numbers of cells that die but not the percentage of cells that die (see Table 2).

### *Application of Heterochrony Theory to Primate Models (Phase 2)*

Through sensitivity analyses of our original model, we have built alternative models, based on the theory of heterochrony, for monkey and human neocortical development. For these alternative models, we hypothesize that the key parameters of neuronogenesis are correlated to the duration of neuronogenesis in each species. These models incorporate the time-extrapolated parameters of the model described above. In addition, they include proportional rate parameters based on the experimental evidence of a decreased cell cycle progression rate during monkey neocortical neuronogenesis compared with mouse neocortical neuronogenesis and the corresponding increased length of the neuronogenesis period in the monkey and human compared with the mouse. As cell cycle kinetics for neocortical neuronogenesis in humans are unavailable, we used this hypothesis to build a model of human neocortical development in which the cell cycle progression rate is proportionally decreased during human neocortical neuronogenesis based on the experimental evidence of the increased length of neocortical neuronogenesis (from 60 to 84 days). Therefore, each time

Downloaded from http://cercor.oxfordjournals.org/ at University of North Texas on January 5, 2017

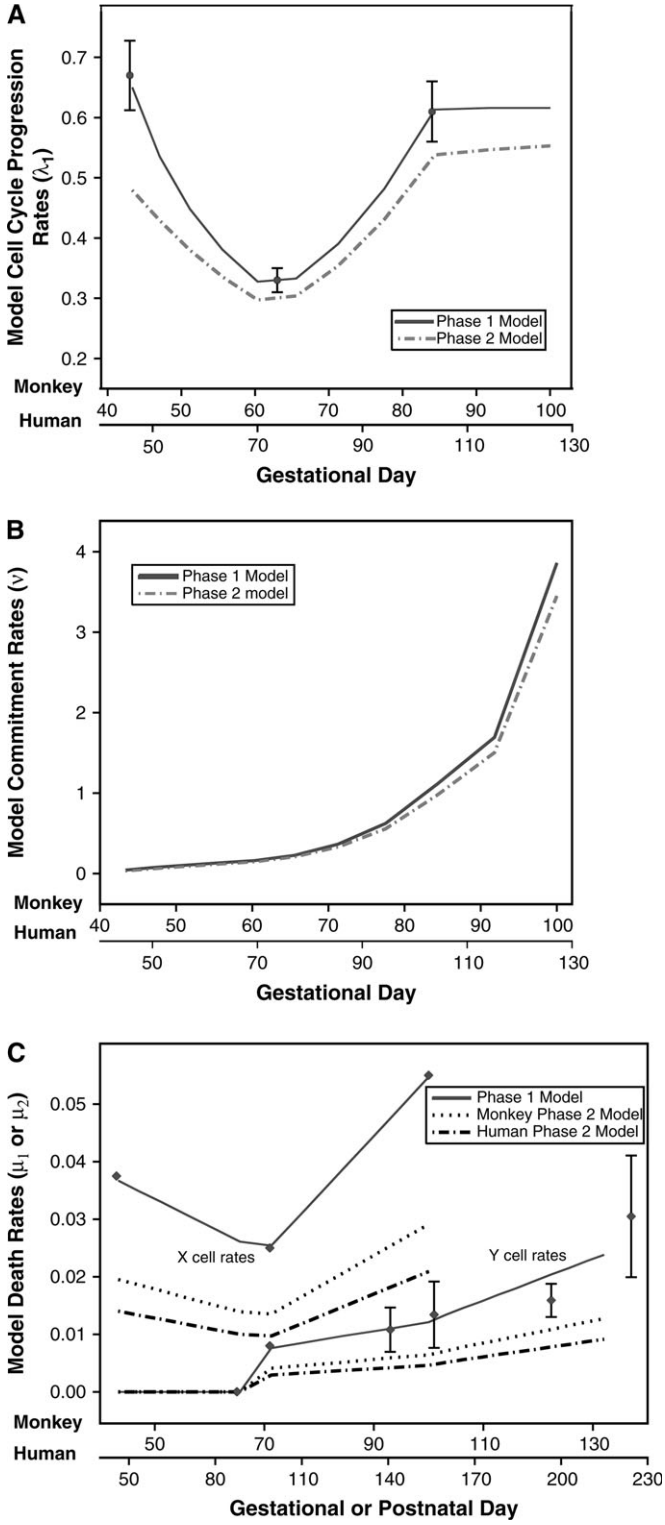


**Figure 3.** Comparison of key time-dependent parameters in Phase 1 and Phase 2 models for human and monkey neocortical neuronogenesis and synaptogenesis. (*A*) Cell cycle progression rates in Phase 1 monkey and human model are directly modeled from the cell cycle length data in the monkey (Kornack and Rakic 1998) shown as solid line, whereas the human Phase 2 model postulates that the increased length of the neuronogenesis period leads to a proportionally increased cell cycle length shown as dashed line (see Eq. 8). (*B*) Commitment rates based on the Phase 1 cell cycle progression rate shown as a solid line versus the commitment rate based on the Phase 2 cell cycle progression rate shown as a dashed line for human and monkey models. (*C*) The solid lines indicate X and Y cell death rates of Phase 1 monkey and human models based on clearance time of TUNEL(+) cells in rat developing neocortex (Thomaidou et al. 1997). Phase 2 models postulate an increased length of cell death based on the increased cell cycle lengths seen in monkeys compared with mice, indicated by the dotted line for the monkey and dashed line for the human Phase 2 models. See Methods section (Eqs. 7, 9, and 10) for further details.

step in the human model was given a new cell cycle progression rate ($\lambda_{hum}^{prop}$) based on the equations below:

$$\lambda_{hum}^{prop}(t_{hum}) = (84/60) \times \lambda_{mon}(t_{mon}), \quad (8)$$

where $t_{mon} = (t_{hum} - 46) \times 60/84 + 40$. This new cell cycle progression rate also decreases the commitment rate slightly based on the decreased cell cycle length (Fig. 3*B*. and see Eqs. 4 and 5 in previous section).

We also determined a proportional cell death rate based on the hypothesis that the cell cycle length and length of cell death are correlated. For the monkey model, we determined a proportional increase in the clearance time of death labeled cells (CL) based on the proportional increase of the cell cycle length during neuronogenesis using the equation below.

$$CL_{mon}^{prop} = CL \times (\lambda_{mou}(t_{mou})/\lambda_{mon}(t_{mon})), \quad (9)$$

where $\lambda_{mou}$ ($t_{mou}$) is the mouse specific cell cycle progression rate shown in Figure 2(*A*) and described elsewhere (Gohlke et al. 2004). For the human proportional model, we determined a proportional death label time based on the increased monkey cell cycle length and the increased length of the human neuronogenesis period described by the equation below.

$$CL_{hum}^{prop} = CL \times (\lambda_{mou}(t_{mou})/\lambda_{mon}(t_{mon})) \times (84/60). \quad (10)$$

Therefore, in this model we increased the experimentally determined duration of dead cell detection by TUNEL of 2.5 h (Thomaidou et al. 1997) to 6.54 h, reflecting the proportional increase in the experimentally derived cell cycle length from the mouse (Takahashi et al. 1995) to the monkey (Kornack and Rakic 1998) and to the assumed proportional increase in the human based on the increased length of the neuronogenesis period. This lengthening of the clearance time parameter is intended to encompass possible lengthening of any part within the cell death process. These new death label times are then used in the cell death rate equation (7) to determine new cell death rates for each time step (Fig. 3*C*).

In our human model, we increased the founder cell population proportional to the increased length of neuronogenesis.

$$X_{hum}^{prop} = (84/60) \times X_{mon}, \quad (11)$$

where $X_{mon}$ is equal to 5 times that of the stereologically determined founder cell population in the mouse (Haydar et al. 2000), based on the estimate of Caviness et al. (1995).

## Results

We have built models of neocortical neuron acquisition in primate species based on time-adjusted application of experimental data in the mouse, monkey, and human (Figs. 4, 5 Phase 1 models). Voracity and reliability of experimental data for parameter estimation are essential for building a computational model. Therefore, we performed several sensitivity analyses to determine the relative impact of uncertainty surrounding individual parameters in the model (see Methods section and Fig. S1). Subsequently, we applied the theory of heterochrony to our models by adjusting the cell cycle progression and death rates when extrapolating experimental data between species (Figs. 4, 5 Phase 2 models). These rate-adjusted models for monkey and human neocortical development specifically associate the decreased cell cycle progression rate during monkey neocortical neuronogenesis compared with mouse neocortical

Downloaded from http://cercor.oxfordjournals.org/ at University of North Texas on January 5, 2017

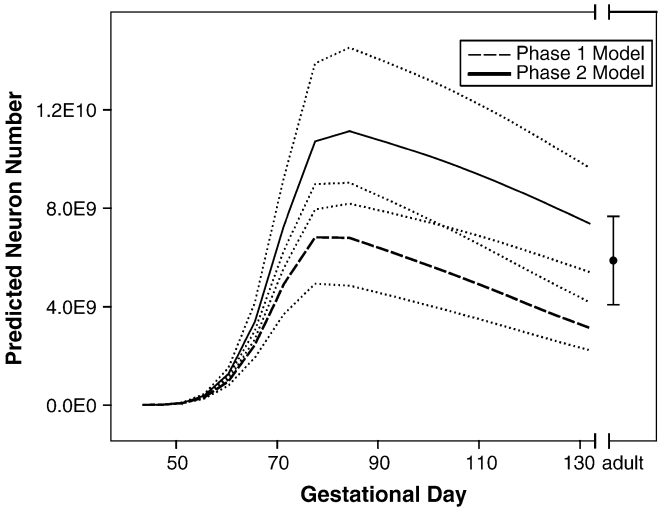


**Figure 4.** Predicted number of neocortical neurons in the rhesus monkey in Phase 1 versus Phase 2 models. The Phase 1 model (dashed line) uses the cell death rate equation based on the clearance time of TUNEL(+) cells of 2.5 h experimentally determined in the developing rat neocortex (Thomaidou et al. 1997). The Phase 2 model (solid line) considers the hypothesis that the length of the neuronogenesis is correlated to the length of the cell cycle and death processes. Therefore, in this model, the clearance time is increased proportional to the experimentally determined increase in the cell cycle length from mouse to monkey (see Eqs. 7 and 9). The dotted lines shown represent predicted 95% population intervals for each model results based on the coefficient of variation reported in the stereological study (approx. 30%). Stereologically determined data on neocortical neuron number (age = 3 years) rhesus monkey are shown for comparison (Lidow and Song 2001). Error bars represent reported standard deviation ($n$ = 4).

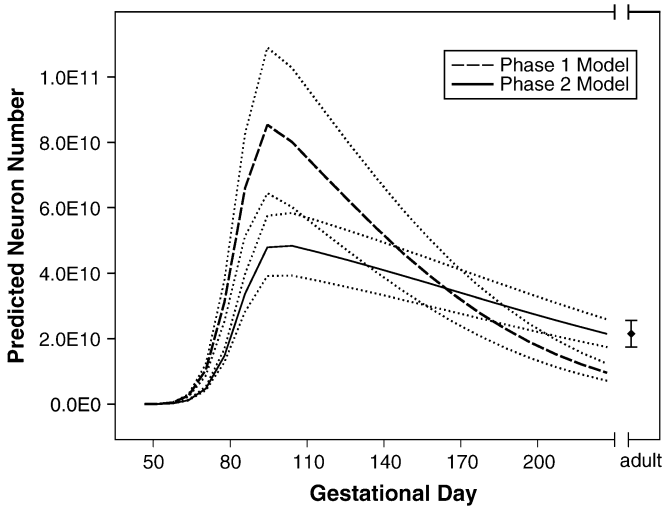


**Figure 5.** Predicted number of neocortical neurons in the human Phase 1 and Phase 2 models. The Phase 1 model (dashed line) uses the cell cycle progression rate of the rhesus monkey model based on the cell cycle length data of Kornack and Rakic (1998) and the cell death rate equation based on the clearance time of TUNEL(+) cells of 2.5 h experimentally determined in the developing rat neocortex (Thomaidou et al. 1997). The Phase 2 model (solid line) considers the hypothesis that the key model parameters such as cell cycle length, cell death rate, and founder cell population is proportional to the length of the neuronogenesis period. Therefore, in this model the human cell cycle was increased proportional to the increased length of the neuronogenesis period based on the proportional increase in cell cycle length from mouse to monkey (see Eq. 8). The clearance time in the cell death rate is also increased proportionally (see Eq. 10). Lastly, the founder cell population ($X_0$) is increased proportional to the increased length of neuronogenesis (Eq. 11). The dotted lines shown represent predicted 95% population intervals of model results based on the coefficient of variation reported in the human stereological study described below (approx. 20%). Stereologically determined data on neocortical neuron number in adult humans are shown for comparison (age range from 20 to 90 years) (Pakkenberg and Gundersen 1997). Error bars represent reported standard deviation ($n$ = 94).

neuronogenesis with an the increased length of the neuronogenesis period in the monkey using a correlation parameter. Therefore, in the human, the cell cycle progression rate is proportionally decreased from the experimentally determined monkey rates based on the increase in the length of the neuronogenesis period from 60 to 84 days (Fig. 3*A*). This increased cell cycle length also affects the commitment rate but only minimally (Fig. 3*B*). For this Phase 2 model, we also determined a proportional cell death rate based on the assumption that the cell cycle length and length of cell death are correlated (Fig. 3*C*).

We compare our Phase 1 model and Phase 2 model output for rhesus monkey neocortical development with independent, stereologically determined neocortical neuron numbers in the adult (Lidow and Song 2001) (Fig. 4). We derived the 95% population intervals of our model simulations based on the reported coefficient of variation of 30% in the stereology study of neocortical cell number in the adult (Lidow and Song 2001). Although the Phase 1 model under predicts the amount of neurons in the adult neocortex, the Phase 2 model, with decreased cell death, provides a better estimate of total neocortical neurons.

Model output for both our Phase 1 and Phase 2 models for human neocortical development through gestational week 32 is shown in Figure 5. We compare our model results with independent stereologically determined neocortical neuron number in adult humans (Pakkenberg and Gundersen 1997). The Phase 1 model, using the cell cycle progression rates of the rhesus monkey and the cell death rates based on the duration of dead cell detection in the developing rodent brain, predicts a large increase of young postmitotic neurons peaking at approximately 16 weeks gestation. After this peak, a rapid decline is evident through 32 weeks of gestation to give a final estimation of approx. 9.6 billion neurons. The Phase 2 model, which has decreased cell cycle progression and death rates based on the hypothesis that these rates are correlated to the increased length of neuronogenesis in humans, predicts a smaller peak of young neurons (approx. 55% of the original model) at 16 weeks. Furthermore, the Phase 2 model predicts a smaller percentage of these young neurons dying through the rest of gestation (approximately 51% compared with 85% in the original model). The final mean neuronal number prediction for the Phase 2 model is 21 billion, which compares well with the independent stereological data in the adult human. As in the monkey, the length of the synaptogenesis period extends beyond 32 weeks of gestation and therefore more cells may die after this point (Rakic et al. 1986). Because no estimates of cell death are available beyond 32 weeks gestation, we do not estimate beyond this point.

Finally, we analyze the contribution of cell death (in proliferative and nonproliferative cell populations) in the shaping of total neuronal number in the neocortex in the 3 modeled species (Table 2). To accomplish this we have applied several quantitative analyses of cell death during neocortical neurogenesis. Our previous simulations on the role of cell death during neuronogenesis and synaptogenesis in the mouse and rat using several experimental datasets suggest that TUNEL results are consistent with other experimental measures of cell death including pyknotic nuclei, Caspase-3 activation, and silver



Downloaded from http://cercor.oxfordjournals.org/ at University of North Texas on January 5, 2017

**Table 2**
Cross-species comparison of the contribution of cell death in models

| | Phase 1 model | Phase 2 model |
|---|---|---|
| Percent cells deleted during neuronogenesis (# of cells in billions)[a] | | |
| Mouse | 10 (0.0021) | — |
| Monkey | 63.7 (9.9) | 35.3 (5.5) |
| Human | 80.5 (257.4) | 48.4 (41.2) |
| Percent cells deleted after neuronogenesis (# of cells in billions)[b] | | |
| Mouse | 21 (0.017) | — |
| Monkey | 44.9 (2.6) | 27.2 (2.8) |
| Human | 84.6 (52.8) | 51.2 (22.5) |

[a]The Y cell output after the last day of neuronogenesis (E16 in mouse, E100 in monkey, and E126 in human) is listed as a percentage and compared with simulations with death rates equal to zero. Total number of cells predicted to die in parentheses in billions.
[b]The Y cell output at the end of modeling period (P14 in mouse, E132 in monkey, E227 in human) compared with the output on the last day of neuronogenesis. Total number of cells predicted to die in parentheses in billions.

staining (Gohlke et al. 2004, 2005). In our current Phase 1 monkey and human models, we predict cell death during neuronogenesis results in cellular loss of 63% and 80%, respectively, whereas our mouse model predicts only a 10% cell loss during neuronogenesis. This is a result of the increased length of the neuronogenesis period in the monkey and human compared with the mouse, as the cell death rate is relatively unchanged across species. Our Phase 2 model works under the hypothesis that the cell death rates ($\mu_1$ and $\mu_2$) are proportionally decreased based on the experimentally determined decreased cell cycle progression rate ($\lambda_1$) in the primate (Kornack and Rakic 1998) compared with the mouse (Miller and Nowakowski 1991; Takahashi et al. 1995). This Phase 2 model predicts less cell loss in the primate species than the Phase 1 model, however, it is still higher than that predicted in the mouse model. Furthermore, both the Phase 1 and Phase 2 models predict more cell loss after neuronogenesis in the primate species than in the mouse (between 27% and 85% in primates compared with 21% in the mouse). Our results suggest that primate species rely more heavily on cell death in shaping the neocortex than rodent species.

## Discussion

We have developed models for the acquisition of neocortical neurons in the rhesus monkey and human and compared these models with independent stereological investigations of neuronal number. We based these models on experimental evidence indicating that the neuronogenesis period and cell cycle length are extended in primate species compared with rodents (Rakic 1974; Miller and Nowakowski 1991; Takahashi et al. 1995; Chan et al. 2002). As experimental data are limited in primate species, we performed sensitivity analyses to determine the overall impact of possible sources of variability in parameter estimation. We explore the impact of correlating the lengthening of the duration of neuronogenesis to the lengthening of individual cellular processes during neuronogenesis including cell cycle progression, commitment, and death rates in primate species compared with rodent species. Through this mathematical application of the evolutionary theory of heterochrony we accurately predict neocortical expansion in primate species.

Compared with previous attempts of modeling neocortical neurogenesis (Polleux et al. 1997; Takahashi et al. 1997; Nowakowski et al. 2002), our mathematical construct is most similar to the compartmentalized structure of Polleux et al. (1997) utilizing the versatility of differential equations to describe the time-dependent nature of neuronogenesis. In addition, our model specifically accounts for cell death in the developing neocortex. The addition of this parameter was previously shown to better predict neuronal numbers in the adult mouse and rat (Gohlke et al. 2002).

### *Alternative Sites of Neocortical Neuronal Generation*

Research has suggested alternative sites of neocortical neuronal generation beyond the VZ. For example, the SVZ, an auxillary proliferative zone derived from the VZ, is thought to give rise to all interneurons in the developing human neocortex (Letinic et al. 2002). Our model construct of neocortical neuronal acquisition suggests that neocortical neuronal number can be predicted solely from proliferation of neural progenitor cells in the VZ. This apparent discrepancy may be explained in part by the fact that neuronal progenitor cells within the SVZ are derived from the VZ and are thought to undergo only one mitosis, at most, before migrating out of the SVZ (Haubensak et al. 2004; Miyata et al. 2004). Two studies estimate the inhibitory neurons generated in the SVZ range from 20% to 30% of the total neocortical neuronal population in rodents and rhesus monkey (Beaulieu et al. 1992; Parnavelas et al. 2000). Alternatively, a study using electron microscopy estimated that only about 12% of interneurons in layers II–VI are derived from the SVZ (Peters 2002).

In order to evaluate the potential impact on our model, we can estimate the maximum number of neurons we may be overlooking by not including those interneurons generated in the SVZ. If we assume that all SVZ progenitor cells originate from the VZ and they undergo one mitosis in the SVZ, then our model would at most not account for half of those neurons generated in the SVZ, suggesting that our mean estimate model may be off by at most 6–15%. This addition would increase our average estimate of total number of neurons to 22–23 billion instead of 21 billion in our human model, which is still well within the range of variability experimentally estimated (15–32 billion) (Pakkenberg and Gundersen 1997). However, based on limited experimental evidence, this assumption could have a different impact on our rodent model, as at least some γ-aminobutyric acidergic interneurons are thought to originate and subsequently migrate from the developing ventral telencephalon (Anderson et al. 1997; Tamamaki et al. 1997).

### *Programmed Cell Death*

Based on our simulations, cell death plays a larger role during primate neocortical development when compared with the mouse. Although the increase in the absolute number of cells predicted to die can be explained in part by the increased founder cell population in primates, as more cells are generated, the predicted percentage of cells that die is also considerably higher in primates versus rodents. Quantitative measurements of TUNEL(+) or pyknotic cells suggest similar percentages of death labeled cells are evident at any one time during human and rodent neocortical development, varying between 0.1% and 0.4% (Hoshino and Kameyama 1988; Thomaidou et al. 1997; Chan and Yew 1998; Haydar et al. 1999; Rakic and Zecevic 2000; Anlar et al. 2003). Some researchers have suggested higher death rates in the proliferative zones (Blaschke et al. 1998), however, these results may be an artifact of the technique used (Gilmore et al. 2000), and are not supported by previous

Downloaded from http://cercor.oxfordjournals.org/ at University of North Texas on January 5, 2017

experiments cited above, experiments using retroviral labeling techniques (Cai et al. 2002), or computational models comparing different techniques for detection of cell death during neocortical neuronogenesis in the mouse and rat (Gohlke et al. 2004).

The total length of neocortical development is much longer in primates than in rodents, whereas the percentage of cells labeled for death is consistent across species; thus we predict more overall cell death in primate species. This prediction is dependent on a constant duration of dead cell label detection for apoptotic cells in all species of 2.5 h based on experiments in the rat model (Thomaidou et al. 1997). Therefore, an alternative explanation is that the cell death process is lengthened concurrently with the lengthening of the cell cycle seen in primate species. In fact, evidence in the rodent suggests the cell death process is intimately connected to the length of the cell cycle as cells only undergo cell death during the G1 phase of the cell cycle (Thomaidou et al. 1997; Liu and Greene 2001). Furthermore, the G1 phase is the most malleable phase of the cell cycle and lengthening of this phase most likely accounts for the longer total cell cycle length in monkeys compared with rodents (Miyama et al. 1997; Caviness et al. 1999; Delalle et al. 1999; Lukaszewicz et al. 2005). Therefore, it is not unreasonable to predict that the cell death rate may be longer in species with longer cell cycle lengths, as we have done in our Phase 2 models, resulting in predictions of less overall cell death and more consistency with stereological data.

Our primate models consider cell death into the third trimester based on data derived from human fetuses through 32 weeks gestation (Chan and Yew 1998; Rakic and Zecevic 2000). We do not know of any other estimates of cell death in primates beyond 32 weeks in the human. However, the synaptogenesis period occurs during the third trimester but then continues at a lower rate after birth in primates (Rakic et al. 1986; Zecevic et al. 1989). Therefore, our model may not account for the total amount of developmentally regulated programmed cell death. However, based on recent stereological evidence, it appears that newborn human infants have comparable numbers of neurons as adults (Larsen et al. 2006), therefore these observations suggest that postnatal neuronal death may be of little consequence to overall neuronal numbers.

### *Heterochrony as a Unifying Evolutionary Theory*

The theory of heterochrony, or changes in the rates and/or the timing of developmental processes, is an important mechanism of evolution (Gould 2000; Kavanagh 2003) and has been used to explain variation in shell size among oysters to brain size and long bone size in mammals (Finlay et al. 1998, 2001; Gould 2000; Cubo et al. 2002; Smith 2006). Although cell cycle lengths vary greatly within species according to the region or developmental process, evidence from the zebrafish, chick, mouse, rat, and the monkey suggests that the average cell cycle length has increased through vertebrate evolution (Jacobson 1991; Miller and Nowakowski 1991; Takahashi et al. 1993; Kornack and Rakic 1998; Li et al. 2000).

The linkage of clock genes, such as beamter/deltaC, and several members of the hairy/E(spl) family, with the Notch signaling pathway (Holley et al. 2000; Julich et al. 2005; Gajewski et al. 2006) may offer genetic support for the theory of heterochrony. Notch signaling is critical for the progression of the cell cycle during neuronogenesis (Bertrand et al. 2002). In fact, it has been suggested that the similar oscillatory gene expression responsible for somitogenesis, may also be critical for the correct patterning of the developing nervous system (Andrade et al. 2005; Freitas et al. 2005).

Clock genes may be involved in regulation of both cell cycle and apoptosis pathways in several tissues (Granda et al. 2004; Okamura 2004; Metz et al. 2006). Experimental research indicates that the cell death process is intimately tied to the cell cycle (Thomaidou et al. 1997; Campagne and Gill 1998; Huard et al. 1999; Liu and Greene 2001; Kendall et al. 2003; Alenzi 2004; Becker and Bonni 2004). For example, researchers have identified that key regulators of apoptosis and the cell cycle, such as p53 and cyclin D2, are closely linked with each other and can coregulate both cell cycle length and apoptosis in the developing brain of the mouse (Campagne and Gill 1998; Huard et al. 1999; Kendall et al. 2003). In addition, evidence suggests that reactivation of genes regulating cell cycle checkpoints, such as Cyclin D2 and E2F, are required for the induction of apoptosis in postmitotic neurons in the CP (Campagne and Gill 1998; Huard et al. 1999; Liu and Greene 2001). Expanding our knowledge of the molecular cascades controlling progenitor cell cycle and cell death will increase our understanding of the underlying evolutionary mechanisms controlling the expansion of the neocortex through primate evolution (Rakic 2005).

The quantitative cross-species comparison of neocortical neuronogenesis described here is critical for identifying predictors of key interspecies differences in the developmental processes underlying neocortical expansion through evolution. Important morphological as well as behavioral attributes associated with the enlarged human neocortex are absent in the primary animal models used in biomedical research in forebrain related diseases such as autism, attention deficit hyperactivity disorder, and schizophrenia. This necessitates quantitative research into the development and evolution of the human neocortex, in order to gain knowledge of our most unique and arguably most valuable feature as humans.

## Supplementary Material

Supplementary material can be found at: http://www.cercor.oxfordjournals.org/.

## Notes

This publication was made possible by grant numbers 2-P01-ES09601 and R01-ES10613 from the National Institute of Environmental Health Sciences (NIEHS), National Institutes of Health (NIH); P30 HD02274 from the National Institute of Child Health and Human Development (NICHD), NIH; RD-83170901, 2W-2296-NATA, and EP05W002745 from the Environmental Protection Agency (EPA); and DE-FG02-03ER63674 from the Department of Energy (DOE). Additional funding was provided by the Center for the Study and Improvement of Regulation at Carnegie Mellon University and the University of Washington. Its contents are solely the responsibility of the author and do not necessarily represent the official views of the NIEHS, NICHD, NIH, EPA, or DOE. *Conflict of Interest*: None declared.

Address correspondence to Elaine M. Faustman, University of Washington, Institute for Risk Analysis and Risk Communication, Department of Environmental and Occupational Health Sciences 4225 Roosevelt Way NE, Suite #100, Seattle, WA 98105-6099, USA. Email: faustman@u.washington.edu.

## References

Alenzi FQB. 2004. Links between apoptosis, proliferation and the cell cycle. Br J Biomed Sci. 61:99–102.



Downloaded from http://cercor.oxfordjournals.org/ at University of North Texas on January 5, 2017

Anderson SA, Eisenstat DD, Shi L, Rubenstein JLR. 1997. Interneuron migration from basal forebrain to neocortex: dependence on Dlx genes. Science. 278:474–476.
Andrade RP, Pascoal S, Palmeirim I. 2005. Thinking clockwise. Brain Res Rev. 49:114–119.
Anlar B, Atilla P, Cakar N, Tombakoglu M, Bulun A. 2003. Apoptosis in the developing human brain: a preliminary study of the frontal region. Early Hum Dev. 71:53–60.
Bayer SA, Altman J, Russo RJ, Zhang X. 1993. Timetables of neurogenesis in the human brain based on experimentally determined patterns in the rat. Neurotoxicology. 14:83–144.
Beaulieu C, Kisvarday Z, Somogyi P, Cyander M, Cowey A. 1992. Quantitative distribution of GABA-immunopositive and -immunonegative neurons and synapses in the monkey striate cortex (area 17). Cereb Cortex. 2:295–309.
Becker EBE, Bonni A. 2004. Cell cycle regulation of neuronal apoptosis in development and disease. Prog Neurobiol. 72:1–25.
Bertrand N, Castro DS, Guillemot F. 2002. Proneural genes and the specification of neural cell types. Nat Rev Neurosci. 3:517–530.
Blaschke AJ, Weiner JA, Chun J. 1998. Programmed cell death is a universal feature of embryonic and postnatal neuroproliferative regions throughout the central nervous system. J Comp Neurol. 396:39–50.
Bruckner G, Mares V, Biesold D. 1976. Neurogenesis in visual system of rat—autoradiographic investigation. J Comp Neurol. 166:245–255.
Cai L, Hayes NL, Takahashi T, Caviness VS, Nowakowski RS. 2002. Size distribution of retrovirally marked lineages matches prediction from population measurements of cell cycle behavior. J Neurosci Res. 69:731–744.
Campagne MV, Gill R. 1998. Tumor-suppressor p53 is expressed in proliferating and newly formed neurons of the embryonic and postnatal rat brain: comparison with expression of the cell cycle regulators p21(Waf1/Cip1), p27(Kip1), p57(Kip2), p16(Ink4a), cyclin G1, and the proto-oncogene Bax. J Comp Neurol. 397:181–198.
Caviness V, Takahashi T, Nowakowski R. 1995. Numbers, time and neocortical neuronogenesis: a general developmental and evolutionary model. Trends Neurosci. 18:379–383.
Caviness VS, Goto T, Tarui T, Takahashi T, Bhide PG, Nowakowski RS. 2003. Cell output, cell cycle duration and neuronal specification: a model of integrated mechanisms of the neocortical proliferative process. Cereb Cortex. 13:592–598.
Caviness VS, Takahashi T, Nowakowski RS. 1999. The G1 restriction point as critical regulator of neocortical neuronogenesis. Neurochem Res. 24:497–506.
Chan WY, Lorke DE, Tiu SC, Yew DT. 2002. Proliferation and apoptosis in the developing human neocortex. Anat Rec. 267:261–276.
Chan WY, Yew DT. 1998. Apoptosis and Bcl-2 oncoprotein expression in the human fetal central nervous system. Anat Rec. 252:165–175.
Chun J. 2000. Cell death, DNA breaks and possible rearrangements: an alternative view. Trends Neurosci. 23:407–408.
Clancy B, Darlington RB, Finlay BL. 2001. Translating developmental time across mammalian species. Neuroscience. 105:7–17.
Clark DA, Mitra PP, Wang SSH. 2001. Scalable architecture in mammalian brains. Nature. 411:189–193.
Cowan WM, Fawcett JW, O'Leary DD, Stanfield BB. 1984. Regressive events in neurogenesis. Science. 225:1258–1265.
Cubo J, Azagra D, Casinos A, Castanet J. 2002. Heterochronic detection through a function for the ontogenetic variation of bone shape. J Theor Biol. 215:57–66.
Dehay C, Giroud P, Berland M, Smart I, Kennedy H. 1993. Modulation of the cell-cycle contributes to the parcellation of the primate visual-cortex. Nature. 366:464–466.
Delalle I, Takahashi T, Nowakowski RS, Tsai LH, Caviness VS. 1999. Cyclin E-p27 opposition and regulation of the G1 phase of the cell cycle in the murine neocortical PVE: a quantitative analysis of mRNA in situ hybridization. Cereb Cortex. 9:824–832.
Faustman EM, Lewandowski TA, Ponce RA, Bartell SM. 1999. Biologically based dose-response models for developmental toxicants: lessons from methylmercury. Inhal Toxicol. 11:559–572.
Finlay BL, Darlington RB. 1995. Linked regularities in the development and evolution of mammalian brains. Science. 268:1578–1584.
Finlay BL, Darlington RB, Nicastro N. 2001. Developmental structure in brain evolution. Behav Brain Sci. 24:263–278.
Finlay BL, Hersman M, Darlington R. 1998. Patterns of vertebrate neurogenesis and paths of vertebrate evolution. Brain Behav Evol. 52:232–242.
Freitas C, Rodrigues S, Saude L, Palmeirim I. 2005. Running after the clock. Int J Dev Biol. 49:317–324.
Gajewski M, Elmasri H, Girschick M, Sieger D, Winkler C. 2006. Comparative analysis of her genes during fish somitogenesis suggests a mouse/chick-like mode of oscillation in medaka. Dev Genes Evol. 216:315–332.
Gilmore EC, Nowakowski RS, Caviness VS, Herrup K. 2000. Cell birth, cell death, cell diversity and DNA breaks: how do they all fit together? Trends Neurosci. 23:100–105.
Gohlke J, Griffith W, Bartell S, Lewandowski T, Faustman E. 2002. A computational model for neocortical neuronogenesis predicts ethanol-induced neocortical neuron number deficits. Dev Neurosci. 24:467–477.
Gohlke J, Griffith WC, Faustman EM. 2004. The role of cell death during neocortical neurogenesis and synaptogenesis: implications from a computational model for the rat and mouse. Dev Brain Res. 151:43–54.
Gohlke JM, Griffith WC, Faustman EM. 2005. A systems-based computational model for dose-response comparisons of two mode of action hypotheses for ethanol-induced neurodevelopmental toxicity. Toxicol Sci. 86:470–484.
Gould SJ. 2000. Of coiled oysters and big brains: how to rescue the terminology of heterochrony, now gone astray. Evol Dev. 2:241–248.
Granda TG, Liu XH, Smaaland R, Cermakian N, Filipski E, Sassone-Corsi P, Levi F. 2005. Circadian regulation of cell cycle and apoptosis proteins in mouse bone marrow and tumor. FASEB J. 19:304–306.
Haubensak W, Attardo A, Denk W, Huttner WB. 2004. Neurons arise in the basal neuroepithelium of the early mammalian telencephalon: a major site of neurogenesis. Proc Natl Acad Sci USA. 101:3196–3201.
Haydar TF, Kuan CY, Flavell RA, Rakic P. 1999. The role of cell death in regulating the size and shape of the mammalian forebrain. Cereb Cortex. 9:621–626.
Haydar TF, Nowakowski R, Yarowsky P, Krueger B. 2000. Role of founder cell deficit and delayed neuronogenesis in microencephaly of the Trisomy 16 mouse. J Neurosci. 20:4156–4164.
Hendry SHC, Jones EG, Emson PC. 1984. Morphology, distribution, and synaptic relations of somatostatin-immunoreactive and neuropeptide y-immunoreactive neurons in rat and monkey neocortex. J Neurosci. 4:2497–2517.
Hofman MA. 1982. Encephalization in mammals in relation to the size of the cerebral cortex. Brain Behav Evol. 20:84–96.
Holley SA, Geisler R, Nusslein-Volhard C. 2000. Control of her1 expression during zebrafish somitogenesis by a Delta-dependent oscillator and an independent wave-front activity. Genes Dev. 14:1678–1690.
Hoshino K, Kameyama Y. 1988. Developmental-stage-dependent radiosensitivity of neural cells in the ventricular zone of telencephalon in mouse and rat fetuses. Teratology. 37:257–262.
Huard JMT, Forster CC, Carter ML, Sicinski P, Ross ME. 1999. Cerebellar histogenesis is disturbed in mice lacking cyclin D2. Development. 126:1927–1935.
Jacobson M. 1991. Developmental neurobiology. New York: Plenum Press.
Julich D, Lim CH, Round J, Nicolaije C, Schroeder J, Davies A, Geisler R, Lewis J, Jiang YJ, Holley SA. 2005. beamter/deltaC and the role of Notch ligands in the zebrafish somite segmentation, hindbrain neurogenesis and hypochord differentiation. Dev Biol. 286:391–404.
Kavanagh KD. 2003. Embedded molecular switches, anticancer selection, and effects on ontogenetic rates: a hypothesis of developmental constraint on morphogenesis and evolution. Evolution. 57:939–948.
Kendall SE, Ryczko MC, Mehan M, Verdi JM. 2003. Characterization of NADE, NRIF and SC-1 gene expression during mouse neurogenesis. Dev Brain Res. 144:151–158.
Kornack DR. 2000. Neurogenesis and the evolution of cortical diversity: mode, tempo, and partitioning during development and persistence in adulthood. Brain Behav Evol. 55:336–344.

Downloaded from http://cercor.oxfordjournals.org/ at University of North Texas on January 5, 2017

Kornack DR, Rakic P. 1998. Changes in cell-cycle kinetics during the development and evolution of primate neocortex. Proc Natl Acad Sci USA. 95:1242–1246.
Larsen CC, Larsen KB, Bogdanovic N, Laursen H, Graem N, Samuelsen GB, Pakkenberg B. 2006. Total number of cells in the human newborn telencephalic wall. Neuroscience. 139:999–1003.
Leroux B, Leisenring W, Moolgavkar S, Faustman EM. 1996. A biologically-based dose-response model for developmental toxicology. Risk Anal. 16:449–458.
Letinic K, Zoncu R, Rakic P. 2002. Origin of GABAergic neurons in the human neocortex. Nature. 417:645–649.
Li Z, Hu M, Ochocinska M, Joseph N, Easter S. 2000. Modulation of cell proliferation in the embryonic retina of zebrafish (Danio rerio). Dev Dyn. 219:391–401.
Lidow MS, Song ZM. 2001. Primates exposed to cocaine in utero display reduced density and number of cerebral cortical neurons. J Comp Neurol. 435:263–275.
Liu DX, Greene LA. 2001. Neuronal apoptosis at the G1/S cell cycle checkpoint. Cell Tissue Res. 305:217–228.
Lukaszewicz A, Savatier P, Cortay V, Giroud P, Huissoud C, Berland M, Kennedy H, Dehay C. 2005. G1 phase regulation, area-specific cell cycle control, and cytoarchitectonics in the primate cortex. Neuron. 47:353–364.
Lund RD, Mustari MJ. 1977. Development of geniculocortical pathway in rats. J Comp Neurol. 173:289–305.
Marin-Padilla M. 1998. Cajal-Retzius cells and the development of the neocortex. Trends Neurosci. 21:64–71.
Metz RP, Qu XY, Laffin B, Earnest D, Porter WW. 2006. Circadian clock and cell cycle gene expression in mouse mammary epithelial cells and in the developing mouse mammary gland. Dev Dyn. 235:263–271.
Miller MW, Kuhn PE. 1995. Cell cycle kinetics in fetal rat cerebral cortex: effects of prenatal treatment with ethanol assessed by a cumulative labeling technique with flow cytometry. Alcohol Clin Exp Res. 19:233–237.
Miller MW, Nowakowski R. 1991. Effect of prenatal exposure to ethanol on the cell cycle kinetics and growth fraction in the proliferative zones of fetal rat cerebral cortex. Alcohol Clin Exp Res. 15:229–232.
Miyama S, Takahashi T, Nowakowski R, Caviness V. 1997. A gradient in the duration of the G1 phase in the murine neocortical proliferative epithelium. Cereb Cortex. 7:678–689.
Miyata T, Kawaguchi A, Saito K, Kawano M, Muto T, Ogawa M. 2004. Asymmetric production of surface-dividing and non-surface-dividing cortical progenitor cells. Development. 131:3133–3145.
Mollgard K, Schumacher U. 1993. Immunohistochemical assessment of cellular proliferation in the developing human CNS using formalin-fixed paraffin-embedded material. J Neurosci Methods. 46:191–196.
Northcutt RG, Kaas JH. 1995. The emergence and evolution of mammalian neocortex. Trends Neurosci. 18:373–379.
Nowakowski R, Lewin S, Miller MW. 1989. Bromodeoxyuridine immunohistochemical determination of the lengths of the cell cycle and the DNA-synthetic phase for an anatomically defined population. J Neurocytol. 18:311–318.
Nowakowski RS, Caviness VS, Takahashi T, Hayes NL. 2002. Population dynamics during cell proliferation and neuronogenesis in the developing murine neocortex. Results Probl Cell Differ. 39:1–25.
Okamura H. 2004. Clock genes in cell clocks: roles, actions, and mysteries. J Biol Rhythms. 19:388–399.
Pakkenberg B, Gundersen HJG. 1997. Neocortical neuron number in humans: effect of sex and age. J Comp Neurol. 384:312–320.
Parnavelas JG, Anderson SA, Lavdas AA, Grigoriou M, Pachnis V, Rubenstein JL. 2000. The contribution of the ganglionic eminence to the neuronal cell types o the cerebral cortex. In: Beck GR, Cardew G, editors. Symposium on Evolutionary Developmental Biology of the Cerebral Cortex. Novartis Foundation 228. London: John Wiley and Sons, Ltd. p. 129–147.
Peters A. 2002. Examining neocortical circuits: some background and facts. J Neurocytol. 31:183–193.
Polleux F, Dehay C, Moraillon B, Kennedy H. 1997. Regulation of neuroblast cell-cycle kinetics plays a crucial role in the generation of unique features of neocortical areas. J Neurosci. 17:7763–7783.
Raff MC, Barres BA, Burne JF, Coles HS, Ishizaki Y, Jacobson MD. 1993. Programmed cell-death and the control of cell-survival—lessons from the nervous-system. Science. 262:695–700.
Rakic P. 1974. Neurons in the monkey visual cortex: systematic relation between time of origin and eventual disposition. Science. 183: 425–427.
Rakic P. 1978. Neuronal migration and contract guidance in primate telencephalon. Postgrad Med J. 54:25–40.
Rakic P. 1988. Specification of cerebral cortical areas. Science. 241:170–176.
Rakic P. 1995. A small step for the cell, a giant leap for mankind: a hypothesis of neocortical expansion during evolution. Trends Neurosci. 18:383–388.
Rakic P. 2005. Less is more: progenitor death and cortical size. Nat Neurosci. 8:981–982.
Rakic P, Bourgeois JP, Eckenhoff MF, Zecevic N, Goldmanrakic PS. 1986. Concurrent overproduction of synapses in diverse regions of the primate cerebral-cortex. Science. 232:232–235.
Rakic P, Kornack DR. 2001. Neocortical expansion and elaboration during primate evolution: a view from neuroembryology. In: Falk D, Gibson KR, editors. Evolutionary anatomy of the primate cerebral cortex. Cambridge: Cambridge University Press.
Rakic S, Zecevic N. 2000. Programmed cell death in the developing human telencephalon. Eur J Neurosci. 12:2721–2734.
Rockel A, Horns R, Powell T. 1980. The basic uniformity of structure of the neocortex. Brain. 103:221–244.
Samuelsen GB, Larsen KB, Bogdanovic N, Laursen H, Graem N, Larsen JF, Pakkenberg B. 2003. The changing number of cells in the human fetal forebrain and its subdivisions: a stereological analysis. Cereb Cortex. 13:115–122.
Simonati A, Rosso T, Rizzuto N. 1997. DNA fragmentation in normal development of the human central nervous system: a morphological study during corticogenesis. Neuropathol Appl Neurobiol. 23:203–211.
Simonati A, Tosati C, Rosso T, Piazzola E, Rizzuto N. 1999. Cell proliferation and death: morphological evidence during corticogenesis in the developing human brain. Microsc Res Tech. 45:341–352.
Smart IHM, Smart M. 1977. The location of nuclei of different labeling intensities in autoradiographs of the anterior forebrain of postnatal mice injected with [3H]thymidine on the eleventh and twelfth days post-conception. J Anat 123 (Pt. 2):515–525.
Smart JL. 1991. Critical periods in brain-development. Ciba Found Symp. 156:109–128.
Smith KK. 2006. Craniofacial development in marsupial mammals: developmental origins of evolutionary change. Dev Dyn. 235: 1181–1193.
Takahashi T, Nowakowski R, Caviness V. 1993. Cell cycle parameters and patterns of nuclear movement in the neocortical proliferative zone of the fetal mouse. J Neurosci. 13:820–833.
Takahashi T, Nowakowski R, Caviness V. 1995. The cell cycle of the pseudostratified ventricular epithelium of the embryonic murine cerebral wall. J Neurosci. 15:6046–6057.
Takahashi T, Nowakowski R, Caviness V. 1996. The leaving or Q fraction of the murine cerebral proliferative epithelium: a general model of neocortical neuronogenesis. J Neurosci. 16:6183–6196.
Takahashi T, Nowakowski R, Caviness V. 1997. The mathematics of neocortical neuronogenesis. Dev Neurosci. 19:17–22.
Tamamaki N, Fujimori KE, Takauji R. 1997. Origin and route of tangentially migrating neurons in the developing neocortical intermediate zone. J Neurosci. 17:8313–8323.
Thomaidou D, Mione MC, Cavanagh JF, Parnavelas JG. 1997. Apoptosis and its relation to the cell cycle in the developing cerebral cortex. J Neurosci. 17:1075–1085.
Verney C, Takahashi T, Bhide P, Nowakowski R, Caviness V. 2000. Independent controls for neocortical neuron production and histogenetic cell death. Dev Neurosci. 22:125–138.
Voyvodic JT. 1996. Cell death in cortical development: how much? Why? So what? Neuron. 16:693–696.
Zecevic N, Bourgeois JP, Rakic P. 1989. Changes in synaptic density in motor cortex of rhesus-monkey during fetal and postnatal life. Dev Brain Res. 50:11–32.

Downloaded from http://cercor.oxfordjournals.org/ at University of North Texas on January 5, 2017